Nanomolar Inhibitors of AmpC β-Lactamase

Federica Morandi,[†] Emilia Caselli,[‡] Stefania Morandi,[‡] Pamela J. Focia,[§]
Jesús Blázquez,[||] Brian K. Shoichet,*,[†] and Fabio Prati*,[‡]

*Contribution from the Department of Pharmaceutical Chemistry, University of California,
San Francisco, Mission Bay Genentech Hall, 600 16th Street, Mail Box 2240,
San Francisco, California 94143, Dipartimento di Chimica, Universitá degli studi di Modena e
Reggio Emilia, via Campi 183, Modena, Italy, Department of Molecular Pharmacology and
Biological Chemistry, Northwestern University, 303 East Chicago Avenue,
Chicago, Illinois 60611, and Servicio de Microbiologia, Hospital Ramón y Cajal,
National Institute of Health (INSALUD), Madrid, Spain*

Received October 5, 2002 ; E-mail: shoichet@cgl.ucsf.edu; prati.fabio@unimore.it

Abstract: β-lactamases are the most widespread resistance mechanism to β-lactam antibiotics, such as the penicillins and the cephalosporins. In an effort to combat these enzymes, a combination of stereoselective organic synthesis, enzymology, microbiology, and X-ray crystallography was used to design and evaluate new carboxyphenyl-glycylboronic acid transition-state analogue inhibitors of the class C β-lactamase AmpC. The new compounds improve inhibition by over 2 orders of magnitude compared to analogous glycylboronic acids, with K_i values as low as 1 nM. On the basis of the differential binding of different analogues, the introduced carboxylate alone contributes about 2.1 kcal/mol in affinity. This carboxylate corresponds to the ubiquitous C3(4)′ carboxylate of β-lactams, and this energy represents the first thermodynamic measurement of the importance of this group in molecular recognition by class C β-lactamases. The structures of AmpC in complex with two of these inhibitors were determined by X-ray crystallography at 1.72 and 1.83 Å resolution. These structures suggest a structural basis for the high affinity of the new compounds and provide templates for further design. The highest affinity inhibitor was 5 orders of magnitude more selective for AmpC than for characteristic serine proteases, such as chymotrypsin. This inhibitor reversed the resistance of clinical pathogens to the third generation cephalosporin ceftazidime; it may serve as a lead compound for drug discovery to combat bacterial resistance to β-lactam antibiotics.

Introduction

Novel compounds are actively pursued as leads for drug discovery. Chemically, novel leads provide insight about the recognition determinants of the target receptor. Biologically, they can have specificities that substrate analogues lack and elude barriers or defenses to which substrate analogues fall victim.

The need for such new biological effects is keenly felt in the search for inhibitors of β-lactamases. These enzymes are the major resistance determinants to β-lactam antibiotics, including the penicillins and the cephalosporins, and threaten public health.[1,2] To combat these enzymes, β-lactam inhibitors such as clavulanic acid, or "β-lactamase resistant" β-lactams such as ceftazidime, have been introduced (Figure 1). The similarity of these β-lactams to the original substrates has allowed resistance to develop further. Broad-spectrum β-lactamases, such as the class C β-lactamase AmpC, have spread among bacteria. Point substitutions have resulted in mutants of once narrow-
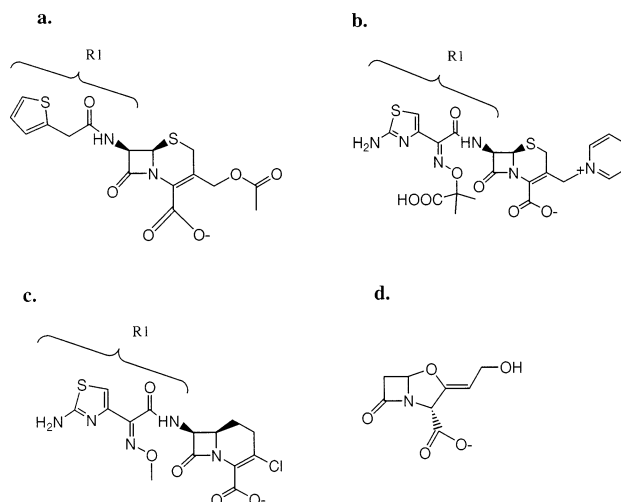
Figure 1. Chemical structures of several β-lactam ligands; the R1 side chains are marked. (a) The substrate cephalothin. (b) The "β-lactamase resistant" ceftazidime. (c) The inhibitor ATMO-carbacephem.[4] (d) The inhibitor clavulanic acid.

spectrum class A β-lactamases, leading to enzymes such as TEM-30 and TEM-64 that are either less inhibited by, or can simply hydrolyze, the "β-lactamase resistant" compounds. Recently, new substrate analogues have been described that can

(1) Matagne, A.; Dubus, A.; Galleni, M.; Frere, J. M. *Nat. Prod. Rep.* **1999**, *16*, 1−19.
(2) Rice, L. B.; Bonomo, R. A. *Drug Resist. Updates* **2000**, *3*, 178−189.

a.

b.

c.
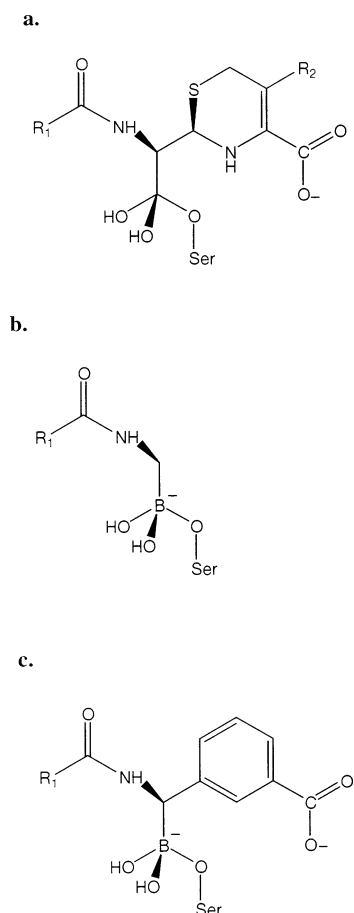
Figure 2. Comparison between the deacylation high energy intermediate of a cephalosporin in a serine β-lactamase (a), a transition-state analogue glycylboronic acid (b), and a transition-state analogue *m*.carboxyphenyl-glycylboronic acid (c).

inhibit these mutant[3] and broad-spectrum β-lactamases[4] with IC$_{50}$ values as low as 100 nM (Figure 1). Given their similarity to substrates, one worries that resistance will rapidly develop against these new agents as well.

A more ambitious strategy abandons substrate information altogether, focusing instead on the structure of the receptor as the sole template for design. Structure-based screening approaches have discovered inhibitors dissimilar to both substrates and substrate analogues.[5,6] These novel inhibitors may evade traditional, pre-evolved resistance mechanisms. Conversely, novel inhibitors of AmpC β-lactamase are relatively weak, with K_i values in the 25 μM range.[6]

Between the extremes of substrate analogues and structure-based discovery lie transition-state analogues (Figure 2),[7−10]

(3) Mourey, L.; Kotra, L. P.; Bellettini, J.; Bulychev, A.; O'Brien, M.; Miller, M. J.; Mobashery, S.; Samama, J. P. *J. Biol. Chem.* **1999**, *274*, 25260−25265.
(4) Trehan, I.; Morandi, F.; Blaszczak, L. C.; Shoichet, B. K. *Chem. Biol.* **2002**, *9*, 1−10.
(5) Toney, J. H.; Fitzgerald, P. M.; Grover-Sharma, N.; Olson, S. H.; May, W. J.; Sundelof, J. G.; Vanderwall, D. E.; Cleary, K. A.; Grant, S. K.; Wu, J. K.; Kozarich, J. W.; Pompliano, D. L.; Hammond, G. G. *Chem. Biol.* **1998**, *5*, 185−196.
(6) Powers, R. A.; Morandi, F.; Shoichet, B. K. *Structure* **2002**, *10*, 1013−1023.
(7) Crompton, I. E.; Cuthbert, B. K.; Lowe, G.; Waley, S. G. *Biochem. J.* **1988**, *251*, 453−459.
(8) Chen, C. C.; Rahil, J.; Pratt, R. F.; Herzberg, O. *J. Mol. Biol.* **1993**, *234*, 165−178.
(9) Strynadka, N. C.; Martin, R.; Jensen, S. E.; Gold, M.; Jones, J. B. *Nat. Struct. Biol.* **1996**, *3*, 688−695.

such as boronic acids. These inhibitors replace the β-lactam recognition motif with a boronic acid, which makes a reversible, dative covalent bond with the active site serine residue forming a tetrahedral adduct (Figure 2a). Replacing the lactam group with a boronic acid makes these inhibitors novel enough to evade many of the resistance mechanisms that now jeopardize β-lactams.[11] By the deployment of side chains normally found in substrates, it has been possible to improve the potency of these compounds, down to 5.9 nM for TEM-1.[9,12] We previously found that glycylboronic acids (Figure 2b) inhibit AmpC competitively, with K_i values as low as 20 nM.[10]
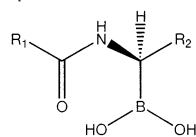
The glycylboronic acids resemble half of the β-lactam molecule, bearing the R1 side chain of substrates but lacking recognition elements corresponding to the thiazolidine or dihydrothiazine rings of penicillins or cephalosporins, respectively (Figure 1a). The absence of a negatively charged group in a position corresponding to the C4′ position of the dihydrothiazine ring seems particularly noteworthy. All β-lactams bear a carboxylic or sulfonic acid at this position. In class A β-lactamases, this group is a key recognition element.[9,12,13] In class C β-lactamases, the role of this group is less understood. Mutant and substrate analyses suggest that such a charged group is not key for recognition.[13] Conversely, structural analyses of the binding determinants ("hot spots") of AmpC suggest that there is a carboxylate binding site on the enzyme.[14] The contribution to binding energy that such a carboxylate might make, if any, remains in doubt, owing to the irreversible binding of β-lactams to β-lactamases, preventing equilibrium-based thermodynamic analyses.

Here, we describe a structure-based approach to the design and testing of *m*.carboxyphenylglycylboronic acids (Figure 2c). The *m*.carboxylate group is meant to correspond to the C4′ carboxylate of cephalosporins in their tetrahedral high-energy intermediate form, mimicking both the distance to the tetrahedral center and the absolute stereochemistry of the chiral carbon. These new compounds improve inhibition by over 2 orders of magnitude compared to analogous glycylboronic acids (Figure 2b) that lack this group. Since these inhibitors bind reversibly to the enzyme, the different K_i values allow for a thermodynamic analysis of affinity. By making small substitutions to the inhibitors, we may understand the contribution of the carboxylic acid to binding (Table 1). The structures of AmpC in complex with two of these inhibitors, determined by X-ray crystallography, allow us to investigate the structural bases for binding. The selectivity of these inhibitors for AmpC versus characteristic serine proteases, which boronic acids are known to inhibit, is considered, as is their efficacy against pathogenic bacteria expressing class C β-lactamases.

We arrive at compounds that inhibit AmpC with K_i values as low as 1 nM. This affinity is realized by adding more and more functional groups stolen from the β-lactam substrates. If novelty really is a virtue for inhibitor discovery, it may be asked whether, in doing so, we have not entered a Faustian bargain. This is a point to which we will return.

(10) Caselli, E.; Powers, R. A.; Blaszczak, L. C.; Wu, C. Y.; Prati, F.; Shoichet, B. K. *Chem. Biol.* **2001**, *8*, 17−31.
(11) Powers, R. A.; Blazquez, J.; Weston, G. S.; Morosini, M. I.; Baquero, F.; Shoichet, B. K. *Protein Sci.* **1999**, *8*, 2330−2337.
(12) Ness, S.; Martin, R.; Kindler, A. M.; Paetzel, M.; Gold, M.; Jensen, S. E.; Jones, J. B.; Strynadka, N. C. *Biochemistry* **2000**, *39*, 5312−5321.
(13) Frere, J. M. *Mol. Microbiol.* **1995**, *16*, 385−395.
(14) Powers, R. A.; Shoichet, B. K. *J. Med. Chem.* **2002**, *45*, 3222−3234.

Table 1. K_i Values of the Glycylboronic Acids against AmpC

Compound	β-lactam analog	R1	R2	K_i (μM)	$\Delta\Delta G^b$ from **1** (kcal/mol)
1	---	-CH₃	---	18.5[a]	0.00
15	---		*(m-carboxyphenyl)*	0.13	2.95
2	Cloxacillin	*(2-chlorophenyl isoxazole methyl)*	---	0.15[a]	2.85
17	Cloxacillin		*(m-carboxyphenyl)*	5.7	0.70
3	Ceftazidime	*(aminothiazole oxime)*	---	0.020	4.04
14	Ceftazidime		*(m-carboxyphenyl)*	N.O.[c]	---
4	Cephalothin	*(thienylmethyl)*	---	0.32[a]	2.40
16	Cephalothin		*(m-carboxyphenyl)*	0.001	5.82
21	Cephalothin		*(phenyl)*	0.035	3.71

[a] These K_i values were determined in 50 mM KPi pH 7.0.[10] The values in Tris are typically 2-fold lower. [b] Differential free energy of binding relative to compound **1**, calculated at 298 K. Values are calculated using $\Delta\Delta G = -RT \ln K_{i,N}/K_{i,1}$, where N represents the compound to which compound 1 is being compared. Positive values indicate improved affinity. [c] Not obtained.

Results

Synthesis. The synthesis of (*R*)-[1-acylamino-1-(3-carboxyphenyl)]methylboronic acids **15**−**17** employed the general strategy developed by Matteson et al (Scheme 1);[15,16] (+)-pinanediol was chosen as a chiral auxiliary to guide the stereochemical course of the Matteson homologation.[17,18] Protection of the carboxy moiety of 3-bromobenzoic acid **5** as the oxazolidine derivative **6**,[12] followed by boronation of the corresponding lithium derivative at −78 °C with B(OCH₃)₃ and *trans*-esterification with (+)-pinanediol, afforded the desired compound **7** (overall yield of 70% from compound **5**). Compound **7** was converted in a "one pot" reaction to compounds **10**−**12** (16−25% overall yield) to avoid the epimerization of the intermediate α-chloro derivative **8**;[15,18] occasionally, compounds **8** and **9** were isolated and characterized. ¹H NMR analysis of compounds **10**−**12**, particularly the diagnostic signals of the amide NH peaks and the H_endo hydrogen of the pinanyl

moiety, showed a greater than 98% diastereoselectivity of the "one pot" reaction.[19,20] All attempts to synthesize **13** and **14** failed, probably because of steric hindrance (see Discussion). Following the same protocol, we obtained compound **20** (Scheme 2) in 56% overall yield, starting from the (+)-pinanediol phenylboronate **19**. The conversion of the pinanediol esters to the free boronic acids **15**−**17** and **21** was achieved through hydrolysis in degassed HCl under reflux for 1 h.[12,21] This treatment also led to the deprotection of the carboxy moiety. Compound **17** was obtained by extraction with EtOAc, and compounds **15**, **16**, and **21** were recovered from the aqueous phase. All compounds were fully characterized by ¹H and ¹³C NMR, IR, mass spectra, and elemental analyses except for compounds **15**−**17** and **21**, for which mass spectra were unobtainable. Nevertheless, the X-ray structures, combined with the NMR and IR analyses, unambiguously identified these compounds.

(15) Matteson, D. S.; Ray, R.; Rocks, R. R.; Tsai, D. J. S. *Organometallics* **1983**, *2*, 1536−1543.
(16) Matteson, D. S. *Acc. Chem. Res.* **1988**, *21*, 294−300.
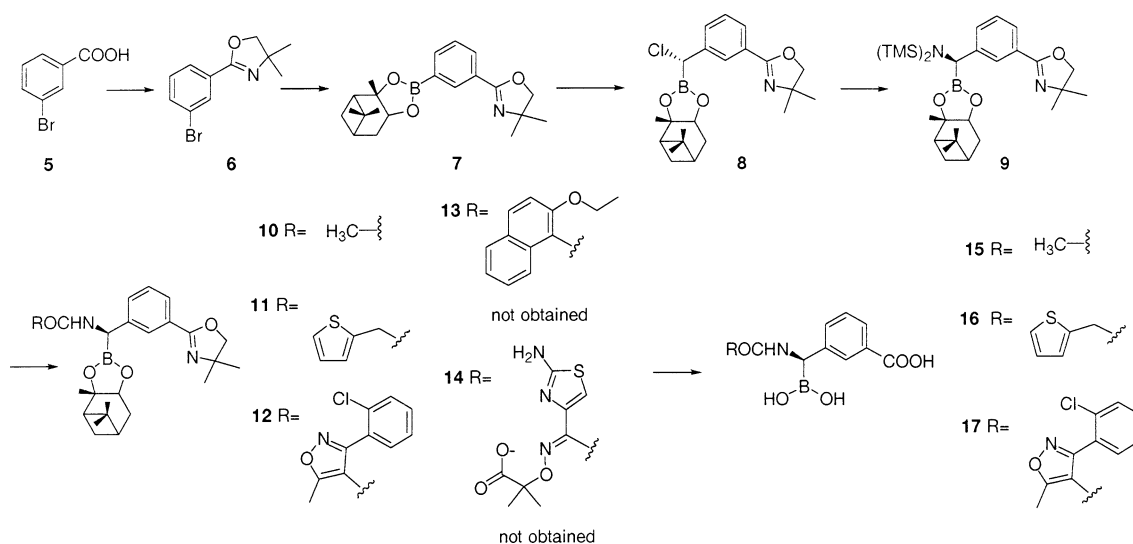(17) Matteson, D. S. *Chem. Rev.* **1989**, *89*, 1535−1551.
(18) Matteson, D. S. *J. Organomet. Chem.* **1999**, *581*, 51−65.
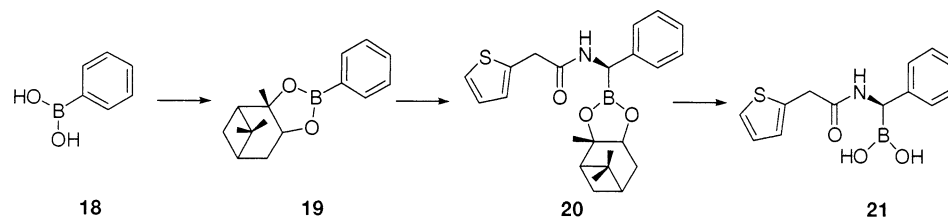(19) Tsai, D. J. S.; Jesthi, P. K.; Matteson, D. S. *Organometallics* **1983**, *2*, 1543−1545.
(20) Matteson, D. S.; Sadhu, K. M.; Peterson, M. L. *J. Am. Chem. Soc.* **1986**, *108*, 810−819.
(21) Martin, R.; Jones, J. B. *Tetrahedron Lett.* **1995**, *36*, 8399−8402.

Scheme 1

5   6   7   8   9

10 R= H₃C—

13 R=
not obtained

11 R=

12 R=

14 R=
not obtained

15 R= H₃C—

16 R=

17 R=

Scheme 2

18   19   20   21

Enzymology and Binding Affinities. All boronic acids inhibitors of AmpC β-lactamase that we have previously studied have been reversible, fast-on fast-off, competitive inhibitors.[10,11,22] The phenylglycylboronic acids, especially the 1 nM inhibitor compound **16**, showed a time-dependent inhibition of AmpC. Notwithstanding this, they were all reversible inhibitors, displaying a classic time-dependent recovery from inhibition during a reaction initiated with substrate (i.e., reaction rates increased after an initial lag phase and then reached a steady-state plateau). The time dependence in the inhibition thus reflects a slow off-rate. Consistent with reversibility, the inhibitors could be competed off by increasing substrate concentration. Perhaps the simplest model to explain the time-dependent effect with these inhibitors is a convolution of their high affinities, a nanomolar K_d value alone would lead to an off-rate on the second time scale, and the dative-covalent nature of the serine–boron bond. There was no significant conformational change in the enzyme site in the complexed structures, suggesting that enzyme reorganization did not present a significant barrier to the inhibitor leaving the site. We have accounted for the incubation effect in the K_i values reported for these inhibitors (see Methods).

To investigate the effect on inhibition of adding an *m*.carboxyphenyl group, we first measured the potency of relatively simple derivatives bearing an acetyl R1 side chain (compound **15**) and an R1 side chain resembling that of cephalothin (compound **16**). These compounds were 150-fold and 300-fold more potent than the lead compounds lacking the *m*.carboxyphenyl side chain, compounds **1** and **4**, respectively

(Table 1). In these compounds, the addition of the *m*.carboxyphenyl side chain improves the binding energy by about 3 kcal/mol.

We reasoned that if we began with better leads than **1** and **4**, which had inhibited AmpC with K_i values of 18.5 and 0.320 μM, respectively,[10] we would achieve still better inhibitors. We therefore turned to the *m*.carboxyphenylglycylboronic acid analogues of compounds **2** and **3**, which had inhibited AmpC with K_i values of 0.150 and 0.020 μM, respectively (Table 1). Surprisingly, compound **17**, bearing the R1 side chain of cloxacillin, was 40-fold less potent (higher K_i) than the original analogue lacking the *m*.carboxyphenyl group (compound **2**). For this compound, the addition of the *m*.carboxyphenyl group made the binding energy about 2 kcal/mol worse (Table 1). We were unable to synthesize the analogue bearing the ceftazidime side chain (**14**).

X-ray Crystallographic Structure Determination. To investigate the structural bases for this dramatic reversal of relative affinities, and to understand detailed recognition, we determined the crystal structure of AmpC in complex with **16** to 1.83 Å resolution (Table 2). Proline and glycine residues excluded, 92.2% of the amino acids were in the most favored regions of the Ramachandran plot (7.8% in the additionally allowed regions).[23]

The position of the inhibitor in the active site was unambiguously identified in the initial $|F_o| - |F_c|$ difference map contoured at 3σ. Electron density connected the Oγ of the catalytic Ser64 to the boron atom of the inhibitors (Figure 3a). The boron geometry was tetrahedral, as expected, and key hydrogen bond interactions in the active site closely resemble

(22) Weston, G. S.; Blazquez, J.; Baquero, F.; Shoichet, B. K. *J. Med. Chem.* **1998**, *41*, 4577–4586.

(23) Laskowski, R. A.; MacArthur, M. W.; Moss, D. S.; Thornton, J. M. *J. Appl. Crystallogr.* **1993**, *26*, 283–291.

Table 2. X-ray Data Collection and Refinement Statistics

	AmpC/**16** complex	AmpC/**21** complex
cell constants (Å; deg)	$a = 117.96; b = 77.49;$	$a = 118.20; b = 76.70;$
	$c = 96.91; β = 115.78$	$c = 97.66; β = 116.31$
space group	C2	C2
resolution (Å)	1.83	1.72
unique reflections	66 946	82 138
total observations	257 829	350 811
R_{merge} (%)	6.0 (42.5)[a]	4.0 (12.0)[a]
completeness (%)	96.5 (91.0)[a]	99.2 (96.0)[a]
$\langle I \rangle / \langle σ(I) \rangle$	19.5 (2.7)[a]	30.0 (11.2)[a]
resolution range for refinement (Å)	20.0−1.83 (1.87−1.83)[a]	20.0−1.72 (1.76−1.72)[a]
number of protein residues	716	716
number of water molecules	468	587
RMSD bond lengths (Å)	0.010	0.014
RMSD bond angles (deg)	1.57	1.76
R_{cryst} (%)	18.7	16.7
R_{free} (%)	21.4	18.9
average B-factor, protein atoms (Å²)	34.8[b]	22.7[b]
average B-factor, inhibitor atoms (Å²)	44.5[b]	36.1[b]
average B-factor, water molecules (Å²)	39.1	34.1

[a] Values in parentheses are for the highest resolution shell. [b] Values cited were calculated for both molecules in the asymmetric unit.

a.

b.
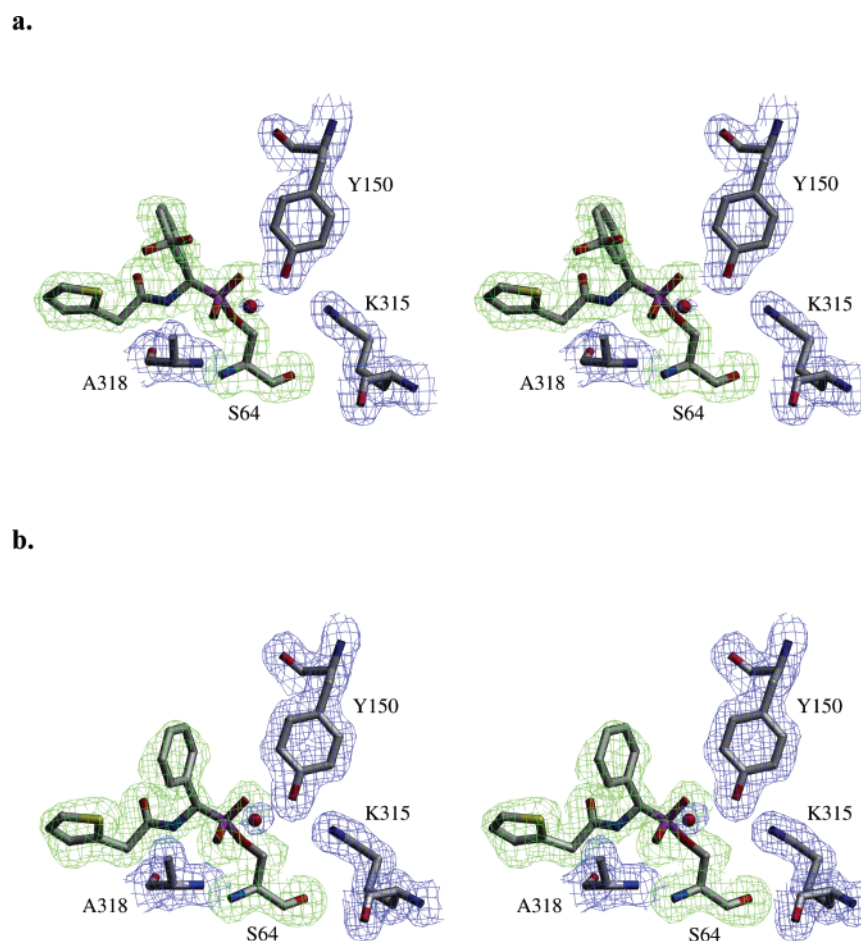
Figure 3. Stereoviews of $2|F_o| − |F_c|$ electron density maps (blue) of the refined model of AmpC in complex with (a) compound **16** and (b) compound **21**, contoured at $1σ$. In green are the simulated-annealing omit electron density maps for the inhibitors, contoured at $3σ$. Carbon atoms are colored gray; oxygen atoms, red; nitrogen atoms, blue; sulfur atoms, yellow; and boron atoms, purple. The putative deacylating water Wat402 is shown as a red sphere. The figures were generated using SETOR.[39]

those typically observed in β-lactamase structures with transition state analogues and with β-lactams (Figure 4a; Table 3).[9,10,12,24,25] The O12 of the boronic acid is placed in the "oxyanion"[26] or

"electrophilic"[25] hole formed by the backbone amide groups of Ser64 and Ala318 (Table 3). The O13 of the boronic acid interacts with the putative catalytic base Tyr150.[24,27] Two well-ordered and highly conserved water molecules are also observed.

(24) Lobkovsky, E.; Billings, E. M.; Moews, P. C.; Rahil, J.; Pratt, R. F.; Knox, J. R. *Biochemistry* **1994**, *33*, 6762−6772.
(25) Usher, K. C.; Blaszczak, L. C.; Weston, G. S.; Shoichet, B. K.; Remington, S. J. *Biochemistry* **1998**, *37*, 16082−16092.

(26) Murphy, B. P.; Pratt, R. F. *Biochem. J.* **1988**, *256*, 669−672.
(27) Dubus, A.; Ledent, P.; Lamotte-Brasseur, J.; Frere, J. M. *Proteins: Struct., Funct., Genet.* **1996**, *25*, 473−485.

a.

b.

c.
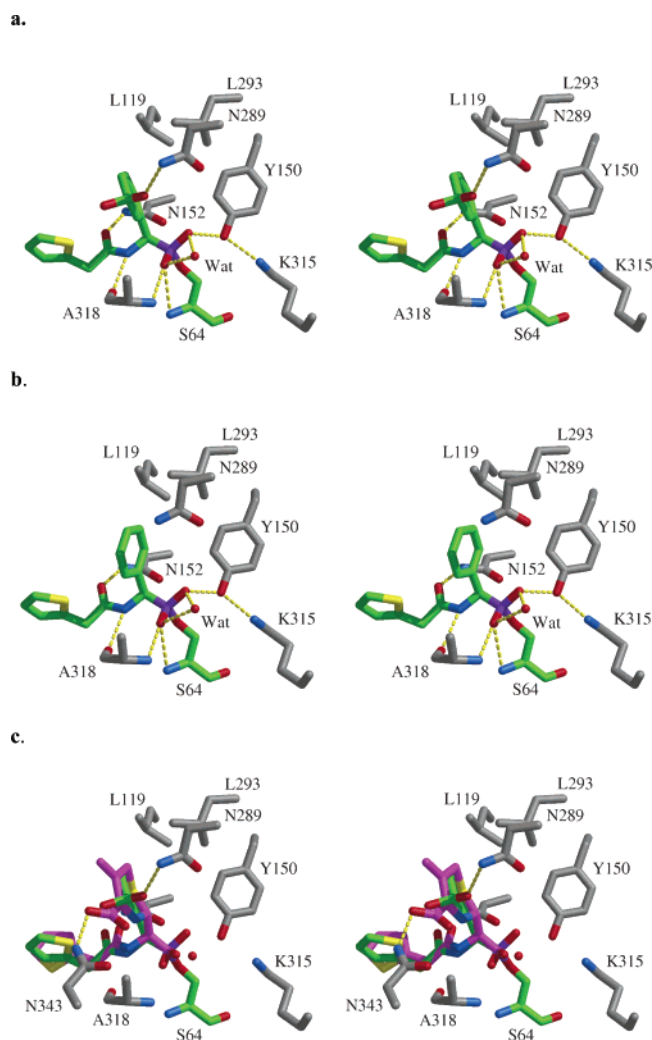
Figure 4. Active site of AmpC in complex with (a) compound **16** and (b) compound **21**. In part c, the complex of AmpC with **16** is overlaid with AmpC in complex with cephalothin (PDB entry 1KVL). Dashed yellow lines represent key hydrogen bonds. Atoms are colored as in Figure 1, except for the inhibitors (**16** and **21**), whose carbon atoms are colored green, and for the substrate cephalothin, whose carbon atoms are colored magenta. Red spheres represent water molecules. Interaction distances are listed in Table 3. Figures 4 and 5 were generated using MidasPlus.[40]

Wat402, which appears to be the deacylating water,[11,28−30] interacts with both O12 and O13 of the boronic acid (Figure 4a). The second water molecule, Wat403, interacts with Wat402, the Oδ1 atom of Asn346, and the Nη1 atom of Arg349 (not shown). The amide group of the inhibitor is placed in the amide recognition region defined by Asn152 and Ala318.[14] The nitrogen (N9) of the amide group interacts with the backbone oxygen of Ala318, and the carbonyl oxygen (O8) interacts with Nδ2 of Asn152. The benzene ring is in van der Waals contact with Leu119 and Leu293 (distances range from 3.6 to 4.5 Å for each leucine, respectively), which form a hydrophobic patch on AmpC.[14] Unexpectedly, the carboxylic acid group is observed to interact with Nδ2 of Asn289 and two ordered water molecules, Wat181 and Wat469. Although canonical carboxylate

(28) Patera, A.; Blaszczak, L. C.; Shoichet, B. K. *J. Am. Chem. Soc.* **2000**, *122*, 10504−10512.
(29) Crichlow, G. V.; Nukaga, M.; Doppalapudi, V. R.; Buynak, J. D.; Knox, J. R. *Biochemistry* **2001**, *40*, 6233−6239.
(30) Beadle, B. M.; Trehan, I.; Focia, P. J.; Shoichet, B. K. *Structure* **2002**, *10*, 413−442.

Table 3. Interactions in Inhibitor Bound and Native AmpC β-Lactamase

16   **21**

	distance (Å)		
interaction	AmpC/**16**[a]	AmpC/**21**[b]	apo[b,c]
S64N−O12	3.1	3.2	N.P.[d]
A318N−O12	2.7	2.8	N.P.
A318O−O12	3.3	3.3	N.P.
Y150OH−O13	2.7	2.7	N.P.
Wat402−O12	2.8	3.0	N.P.
Wat402−O13	3.0	2.9	N.P.
Y150OH−K315Nξ	2.9	2.9	2.5
Y150OH−S64Oγ	3.0	3.0	3.2
Y150OH−K67Nξ	3.3	3.2	3.1
K67Nξ−A220O	2.8	2.9	3.5
K67Nξ−S64Oγ	2.6	2.7	3.5
Wat402−T316Oγ1	3.4	3.2	3.8
Wat402−Wat403	2.6	2.7	2.9
Wat403−N346Oδ1	2.7	2.8	2.7
Wat403−R349Nη1	3.0	3.1	2.9
A318O−N9	3.1	3.2	N.P.
N152Nδ2−O8	2.8	2.9	N.P.
Q120Nε2−O8	6.5	2.9	N.P.
N152Oδ1−K67Nξ	2.6	2.6	2.7
N152Nδ2−Q120Oε1	7.1	2.6	3.0
Wat181−O22	3.0	N.P.	N.P.
Wat469−O23	3.1	N.P.	N.P.
N189Nδ2−O22	2.9	N.P.	N.P.

[a] Distances are for monomer 1 of the asymmetric unit. [b] Distances are for monomer 2 of the asymmetric unit. [c] The apo structure used as reference is PDB code 1KE4.[14] [d] Not present.

binding residues, such as Thr316 and Asn346, are nearby, no direct interaction is observed to these residues.

To investigate the role of this carboxylate, the derivative **21** was made, lacking the carboxylate but maintaining the phenyl ring. This compound was 35-fold less active than compound **16**, which has the carboxylate (Table 1). Comparing the affinity of **21** (K_i value of 35 nM) to the affinity of **16** (K_i value of 1 nM) suggests that the carboxylate by itself contributes about 2.1 kcal/mol to the interaction energy with AmpC.

To understand this result, we determined the crystal structure of AmpC in complex with **21** to 1.72 Å resolution. Proline and glycine residues excluded, 92.5% of the amino acids were in the most favored regions of the Ramachandran plot (7.5% in the additionally allowed regions),[23] with other crystallographic statistics consistent with a well-determined structure (Table 2). The position of the inhibitor in the active site was unambiguously identified in the initial $|F_o| - |F_c|$ difference map contoured at 3σ. Electron density connected the Oγ of the catalytic Ser64 to the boron atom of the inhibitor; the boron geometry was tetrahedral, as expected (Figure 3b). The AmpC/**21** complex resembles the AmpC/**16** complex, making the most of the same interactions, save for those involving the deleted carboxylate group (Figure 4b, Table 3).

Microbiology. To investigate the potential of these compounds to reverse antibiotic resistance, we undertook preliminary antimicrobial activity studies in bacterial cell culture. The minimum inhibitory concentration (MIC) of ceftazidime against eight clinically isolated bacterial pathogens producing class C

Table 4. Synergy of Compounds **16** and **21** with Ceftazidime against Bacteria Producing β-Lactamase

	MIC[a] (μg/mL)		
strain	CAZ[b]	CAZ + **16**[b,c]	CAZ + **21**[b,c]
C. freundii	256	8	8
E. coli 1[d]	32	1	4
E. coli 2[d]	256	16	16
E. cloacae 1[d]	256	8	8
E. cloacae 2[d]	32	4	8
E. cloacae 3[d]	256	16	16
P. aeruginosa 1[d]	256	16	32
P. aeruginosa 2[d]	64	8	8

[a] Minimum inhibitory concentration. [b] CAZ = ceftazidime. [c] The ratio of ceftazidime to inhibitor was 1:1. [d] Strains defined in Materials and Methods.

Table 5. Selectivity of **16** and **21** for AmpC versus Serine Proteases

enzyme	IC$_{50}$ (μM) for **16**	IC$_{50}$ (μM) for **21**
AmpC	0.0026	0.090
α-chymotrypsin	150	6.0
β-trypsin	≫1000	≫1000
elastase	500	128

β-lactamases ranged from 256 μg/mL to 32 μg/mL. Both **16** and **21** showed synergy with ceftazidime against all strains. Compound **16** was slightly more potent than compound **21**, improving the MIC values of ceftazidime by between 8- and 32-fold (Table 4).

Selectivity. To investigate the selectivity of these compounds, **16** and **21** were tested against the serine proteases α-chymotrypsin, β-trypsin, and elastase (Table 5). Compound **16** was 57 000-fold more selective for AmpC over α-chymotrypsin and 190 000-fold more selective for AmpC over elastase. Compound **21** was 60-fold and 1400-fold more selective for AmpC over α-chymotrypsin and elastase, respectively. Neither compound had any measurable activity against β-trypsin below 1 mM.

Discussion

The aspect of this study that first attracted our attention was the high affinity of compound **16**, which inhibits AmpC β-lactamase with a K_i value of 1 nM (Table 1). This is a 300-fold improvement over the parent compound **4** (Table 1), which lacks the *m.*carboxyphenyl group.[10] This result supports the view that a C3(4)′ acidic group, which is ubiquitous among β-lactams, is a key recognition feature in AmpC. Although this is well accepted for the class A β-lactamases, the contribution of the β-lactam carboxylate to recognition by the class C enzymes has been uncertain.[13] It is appropriate to consider what enzyme groups are responsible for complementing this functionality.

To answer this question, we determined the structure of the complex between AmpC and compound **16** by X-ray crystallography (Figure 4a, Table 2). We expected to see the carboxylate of **16** interact with Asn346 or Thr316, which both crystallography and mutagenesis studies suggest are responsible for interacting with the C3(4)′ carboxylates of penicillins and cephalosporins.[24,28−30] Instead, we found that the carboxylate hydrogen bonded with the nearby Asn289 and two ordered water molecules new to this structure (Figure 4a and c; Table 3). Asn289, though in the active site region, has not previously been implicated as a functional residue in AmpC and is only modestly conserved among class C β-lactamases (although in

most species of AmpC a polar residue is found at this position). This led us to wonder if the carboxylate was really driving affinity and not some other group. For instance, the phenyl ring of the *m.*carboxyphenyl group formed van der Waals interactions with the hydrophobic patch on AmpC made up of Leu119 and Leu293, previously found to be a hot spot for ligand interactions in the enzyme.[14] Perhaps it was the phenyl ring, not the carboxylate, that was responsible for the nanomolar inhibition of compound **16**.

To investigate this possibility, we synthesized compound **21**, the analogue of **16** that retains the phenyl ring but replaces the *m.*carboxylate with a hydrogen (Table 3). If the phenyl ring was responsible for most of the 3.4 kcal/mol improvement in interaction energy, we would expect the affinity of this analogue to resemble that of **16**. Instead, it lost 35-fold activity compared to **16**, suggesting that the carboxylate is responsible for most of the affinity gain (Table 1). The structure of the AmpC/**21** complex, determined by X-ray crystallography to 1.72 Å, shows that the two compounds bind similarly in the AmpC site and that no significant enzyme rearrangement has occurred between the two complexes.

This returns us to the original premise that the carboxylate is a key recognition feature for AmpC. Since the phenylglycylboronic acids are reversible inhibitors, we can for the first time assign an energetic value to having this functional group: 2.1 kcal/mol. This is a large value, considering the need to desolvate the carboxylate, though not unprecedented for a polar-ionic interaction.[31] Whether this energy owes directly to the hydrogen bond between the carboxylate and Asn289, or to more general interactions with the residues in the carboxylate binding site (Figure 4c),[24,28−30,32] must await protein mutagenesis studies.[31] What is clear now is that this carboxylate contributes significantly to the binding of this inhibitor, and by extension to the recognition of β-lactam substrates by class C β-lactamases.

It is appropriate to ask then why, if the carboxylate contributes so much to binding affinity, is the *m.*carboxyphenylglycylboronic acid **17** such a poor inhibitor, nearly 40-fold *worse* than its analogous glycylboronic acid **2**, the latter of which lacks the carboxylate? An overlay of the crystal structures of the AmpC complex with the glycylboronic acid **2**[10] and that of AmpC/**16** explains this unanticipated drop in affinity (Figure 5). The bulky R1 side chains of **2** and **17**, which bend back toward the boronic acid group, will sterically clash with the introduced *m.*carboxyphenyl moiety in **17**, disrupting its interactions with the enzyme; this would also be true of **14**.[4,33] The inability to even synthesize the *m.*carboxyphenylglycylboronic acid **14**, an analogue of the 20 nM glycylboronic acid **3**,[10] presumably also reflects this crowding. This was disappointing, as we had (naively) hoped that **14** would see the same improvement as **16**, reaching a K_i better than 100 pM. When transition-state analogues are being designed for β-lactamases, care must be taken that the two side chains, each of which individually can contribute significantly to binding, are sterically consistent with one another.

(31) Fersht, A. R.; Shi, J.; Knill-Jones, J.; Lowe, D. M.; Wlkinson, A. J.; Blow, D. M.; Brick, P.; Carter, P.; Waye, M. M. Y.; Winter, G. *Nature* **1985**, *314*, 235−238.
(32) Oefner, C.; D'Arcy, A.; Daly, J. J.; Gubernator, K.; Charnas, R. L.; Heinze, I.; Hubschwerlen, C.; Winkler, F. K. *Nature* **1990**, *343*, 284−288.
(33) Powers, R. A.; Caselli, E.; Focia, P. J.; Prati, F.; Shoichet, B. K. *Biochemistry* **2001**, *40*, 9207−9214.
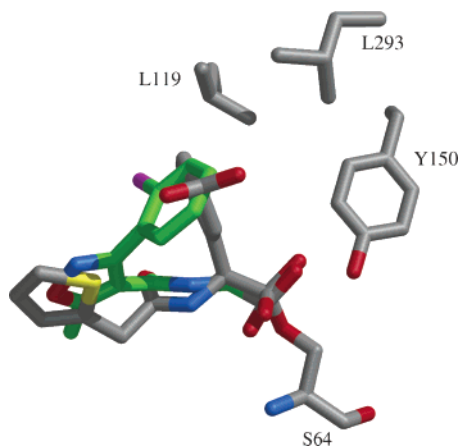
Figure 5. Overlay of the AmpC/**16** and AmpC/**2** complexes (PDB entry 1FSY for AmpC/**2**),[10] each determined by X-ray crystallography. Carbon atoms of **16** are colored gray, and carbon atoms of **2** are colored green.

Even with this caveat, compounds of this family have several attractive features. Compound **16** is highly selective for AmpC, having little affinity for serine proteases such as chymotrypsin (Table 5). This high level of selectivity may reflect the hydrophilicity of compound **16** and its chiral display of relatively dense functionality. Whereas the activity of these compounds in cell culture (Table 4) is several orders of magnitude worse than their activity as enzyme inhibitors, they are nevertheless relatively potent at reversing the resistance of clinical pathogens such as *E. cloacae*, which are currently such a problem in hospitals.

We return, then, to the question raised in the Introduction: how novel is this series, and what are its prospects as antiresistance agents; will resistance easily arise against it? After all, the increased affinity of the transition-state analogues has been achieved through a series of raids on the β-lactam arsenal, resulting in compounds that, except for their boronic acid group, are by now looking rather like β-lactams.

Two views may be considered. The first suggests that resistance will be hardest to develop against analogues that most closely resemble substrates. To achieve resistance, an enzyme must distinguish between the inhibitor and the substrate, since it must still act on the latter, and the more the inhibitor resembles the substrate, the more difficult this will be. In this model, transition-state analogues such as compound **16** increasingly resemble the substrate, while remaining impervious to hydrolysis, and should be difficult to develop resistance against.

A second view recalls that most bacterial resistance mechanisms are ancient in the biosphere and preadapted to recognize an antibiotic class. In the case of β-lactams, these mechanisms include receptors that bind β-lactams and up-regulate β-lactamases, the deletion of porin channels through which β-lactams diffuse, and point mutants, such as those in TEM and SHV β-lactamases, that reduce affinity for β-lactam inhibitors such as clavulanate. In this model, the more a β-lactamase inhibitor resembles a β-lactam, the more subject it will be to these pre-evolved resistance mechanisms.

In this work, we have used stereoselective organic synthesis, enzymology, microbiology, and X-ray crystallography to design *m*.carboxyphenylglycylboronic acids that inhibit class C β-lactamases with K_i values as low as 1 nM. As reversible inhibitors, these molecules probe the recognition determinants of β-lac-

tamases, providing energetic values for interactions observed in the structures of their complexes and by extension those of β-lactams. These crystal structures are templates for yet further improvement in the potency of this family of inhibitors. Whether such potency can be converted into therapeutic use as antiresistance agents will depend at least partly on whether their similarity to substrates makes them more or less sensitive to existing resistance mechanisms. This consideration may bear upon the design of many antiresistance therapeutics; studies to address it are only now beginning.

Materials and Methods

Synthesis and Analysis. All reactions were performed under argon using oven-dried glassware. Solvents were dried according to classical procedures. A cold bath at −100 °C was prepared by addition of liquid nitrogen to a precooled (−80 °C) mixture of 1:1 EtOH/MeOH. Chromatographic purification of the compounds was performed on silica gel (0.05−0.20 mm). Melting points were obtained on a Büchi 510 apparatus and are uncorrected. Optical rotations were recorded at 20 °C on a Perkin-Elmer 241 polarimeter and are in 10^{-1} deg cm^2 g^{-1}. IR spectra were determined in KBr pellets (for solids) and films (for liquids) on a Perkin-Elmer 1600 Series spectrophotometer. ^{1}H and ^{13}C NMR spectra were recorded on a Bruker DPX-200 (at 200 and 50 MHz, respectively) spectrometer: chemical shifts are reported in δ values from TMS as the internal standard. Mass spectra were determined on a Finnigan MAT SSQ A mass spectrometer (EI, 70 eV). Elemental analyses were performed on a Carlo Erba Elemental Analyzer 1110. 2-(3-Bromophenyl)-4,4-dimethyl-4,5-dihydro-oxazole (**6**) was synthesized as described.[12]

(+)-Pinanediol 3-(4,4-Dimethyl-4,5-dihydro-oxazol-2-yl)phenyl-boronate (7). *n*-BuLi (2.5 mL of a 2.5 M solution in hexane, 6.23 mmol) was added dropwise with stirring to a solution of **6** (1.51 g, 5.93 mmol) in THF (9.5 mL) at − 78 °C under argon. After 30 min, a solution of trimethylborate (0.7 mL, 5.93 mmol) in THF (2 mL) was added, and the mixture was stirred for 1.5 h; thereafter, the resulting yellow solution was quenched with TMSCl (0.75 mL, 5.93 mmol) and allowed to reach rt. After 1 h, (+)-pinanediol (1.01 g, 5.93 mmol) dissolved in a minimum amount of anhydrous Et$_2$O was added as one portion to the solution and then stirred overnight. The reaction mixture was partitioned in Et$_2$O (16 mL) and H$_2$O (10 mL), and the aqueous phase was extracted with Et$_2$O (2 × 10 mL). The combined organic phases were dried on MgSO$_4$, filtered, and concentrated to give an orange oil, which was purified by chromatography (7:3 EtPet/EtOAc) and crystallization (EtPet), affording **7** (1.14 g, 54%) as a white crystalline solid, mp 98−101 °C, [α]$_D$ = +11.2 (*c* 1.5, CHCl$_3$). IR (KBr): 1646 cm^{-1}. ^{1}H NMR (CDCl$_3$): δ 0.81 (3H, s, pinanyl CH_3), 1.22 (1H, d, *J* = 10.5 Hz, pinanyl H_{endo}), 1.33 (3H, s, pinanyl CH_3), 1.40 (6H, s, 2CH_3), 1.50 (3H, s, pinanyl CH_3), 1.5−2.5 (5H, m, pinanyl protons), 4.22 (2H, s, CH_2O), 4.47 (1H, dd, *J* = 8.8, 2.0 Hz, pinanyl CHOB), 7.43 (1H, t, *J* = 7.7 Hz, H_5 arom.), 7.92 (1H, dt, *J* = 7.7, 1.5 Hz, H_6 arom.), 8.05 (1H, dt, *J* = 7.7, 1.5 Hz, H_4 arom.), 8.43 (1H, br s, H_2 arom.). ^{13}C NMR (CDCl$_3$): δ 24.4, 26.9, 27.5, 28.8 (2C), 29.1, 35.9, 38.6, 40.0, 51.9, 68.0, 78.8, 79.5, 86.8, 128.1, 131.2, 135.0, 137.8, 162.5 (*C*B and aromatic quaternary *C* not seen). EIMS: *m/z* 353 (M$^+$), 338 (base peak), 323, 282, 242, 202, 186, 130, 103, 67, 55. Anal. Calcd for C$_{21}$H$_{28}$NO$_3$B: C, 71.39; H, 7.99; N, 3.96. Found: C, 71.01; H, 8.65; N, 3.89.

One Pot General Procedure for the Synthesis of (+)-Pinanediol (1*R*)-1-Acylamino-1-[3-(4,4-dimethyl-4,5-dihydro-oxazol-2-yl)phen-yl]methylboronate (10−12). Dichloromethyllithium was generated by adding *n*-BuLi (1.24 mL of a 2.5 M solution in hexane, 3.11 mmol) dropwise to a solution of CH$_2$Cl$_2$ (0.29 mL, 4.53 mmol) in THF (10 mL) with stirring at −100 °C under argon: toward the end of the BuLi addition, precipitation of the white microcrystalline LiCHCl$_2$ became

evident. After 30 min, the mixture was treated with the above pinanediol boronate **7** (1.00 g, 2.83 mmol) and allowed to reach rt with stirring. The tetrahedral boronate adduct precipitated as an abundant white solid at −80 °C and redissolved upon warming. After 1 h at 0 °C, the solution was cooled to −78 °C; LiN(TMS)$_2$ (3.11 mL of a 1 M solution in THF, 3.11 mmol) was added, and the resulting solution was allowed to warm gradually to 20 °C and stirred overnight. The desilylation, acylation, and purification of the product were carried out as described for compounds **10**−**12**.

Analytical samples of compounds **8** and **9** were prepared and characterized.

(+)-Pinanediol (1*S*)-1-Chloro-1-[3-(4,4-dimethyl-4,5-dihydro-oxazol-2-yl)phenyl]methylboronate (**8**): [α]$_D$ = +3.5 (*c* 2.3, CHCl$_3$). IR (film): 1650 cm^{-1}. ^{1}H NMR (CDCl$_3$): δ 0.86 (3H, s, pinanyl C*H*$_3$), 1.17 (1H, d, *J* = 10.5 Hz, pinanyl *H*$_{endo}$), 1.31 (3H, s, pinanyl C*H*$_3$), 1.41 (6H, s, 2C*H*$_3$), 1.43 (3H, s, pinanyl C*H*$_3$), 1.5−2.5 (5H, m, pinanyl protons), 4.13 (2H, s, C*H*$_2$O), 4.41 (1H, dd, *J* = 8.8 Hz, 2.0, pinanyl C*H*OB), 4.58 (1H, br s, C*H*B), 7.41 (1H, t, *J* = 7.7 Hz, *H*$_5$ arom.), 7.64 (1H, dt, *J* = 7.7, 1.5 Hz, *H*$_6$ arom.), 7.88 (1H, dt, *J* = 7.7, 1.5 Hz, *H*$_4$ arom.), 8.02 (1H, t, *J* = 1.5 Hz, *H*$_2$ arom.). ^{13}C NMR (CDCl$_3$): δ 24.3, 26.6, 27.4, 28.7 (3*C*), 35.6, 38.6, 39.7, 45.0 (br, *C*B), 51.7, 67.7, 79.3, 79.6, 87.5, 128.1, 128.6, 129.0, 131.7, 139.6, 162.2. EIMS: *m/z* 401−403 (M$^+$), 386−388, 371−373, 250−252, 223−225 (base peak), 189, 135, 93, 67, 55.

(+)-Pinanediol (1*R*)-1-(*N*-Bistrimethylsilylamino)-1-[3-(4,4-dimethyl-4,5-dihydro-oxazol-2-yl)phenyl]methyboronate (**9**). [α]$_D$ = −2.7 (*c* 2.0, CHCl$_3$). IR (film): 1650 cm^{-1}. ^{1}H NMR (CDCl$_3$): δ 0.13 (18H, 2Si-(C*H*$_3$)$_3$), 0.89 (3H, s, pinanyl C*H*$_3$), 1.30 (1H, d, *J* = 10.5 Hz, pinanyl *H*$_{endo}$), 1.35 (3H, s, pinanyl C*H*$_3$), 1.41 (6H, s, 2C*H*$_3$), 1.46 (3H, s, pinanyl C*H*$_3$), 1.5−2.5 (5H, m, pinanyl protons), 4.12 (2H, s, C*H*$_2$O), 4.14 (1H, br s, C*H*B), 4.39 (1H, dd, *J* = 8.8, 2.0 Hz, pinanyl C*H*OB), 7.33 (1H, t, *J* = 7.7 Hz, *H*$_5$ arom.), 7.62 (1H, dm, *J* = 7.7 Hz, *H*$_4$ arom.), 7.79 (1H, dm, *J* = 7.7 Hz, *H*$_6$ arom.), 8.05 (1H, m, *H*$_2$ arom.). ^{13}C NMR (CDCl$_3$): δ 2.8 (6*C*), 24.4, 26.9, 27.4, 28.7 (3*C*), 35.8, 38.6, 39.9, 47.0 (br, *C*B), 51.9, 67.8, 79.0, 79.4, 86.5, 125.8, 127.1, 127.6, 127.9, 129.7, 145.587, 163.1. EIMS: *m/z* 526 (M$^+$), 511, 453, 275, 203, 135, 130, 93, 73 (base peak), 67, 55.

(+)-Pinanediol (1*R*)-1-Acetylamino-1-[3-(4,4-dimethyl-4,5-dihydro-oxazol-2-yl)phenyl]methylboronate (**10**). After 16 h at rt, the reaction mixture containing the silylamino derivative **9** was cooled at −78 °C and treated with a solution of Ac$_2$O (1.13 mL, 12.00 mmol) and AcOH (194 μL, 3.40 mmol) in THF (2 mL), and then was allowed to warm to rt and stirred overnight. The solution was partitioned in EtOAc (60 mL) and H$_2$O (12 mL), and the aqueous phase was extracted with EtOAc (2 × 15 mL). The combined organic phases were washed with 5% NaHCO$_3$, H$_2$O (6.5 mL), and saturated NaCl (6.5 mL), dried (MgSO$_4$), and concentrated in vacuo to give a brownish oil which was purified by chromatography (95:5 Et$_2$O/MeOH) and crystallization (EtOAc), affording **10** (291 mg, 24% overall yield from **7**) as a white solid, mp 196 °C, [α]$_D$ = −136.9 (*c* 2.1, CHCl$_3$), de > 98%. IR (KBr): 1648, 1600 cm^{-1}. ^{1}H NMR (CDCl$_3$): δ 0.80 (3H, s, pinanyl C*H*$_3$), 1.22 (9H, br s, 2C*H*$_3$−pinanyl C*H*$_3$), 1.32 (3H, s, pinanyl C*H*$_3$), 1.39 (1H, d, *J* = 10.5 Hz, pinanyl *H*$_{endo}$), 1.5−2.5 (8H, m, pinanyl protons and C*H*$_3$CONH at 2.16, d, *J* = 0.67 Hz), 3.92 (1H, br s, C*H*B), 4.05 (3H, m, pinanyl C*H*OB−C*H*$_2$O), 7.28 (2H, m, *H*$_5$−*H*$_6$ arom.), 7.68 (2H, m, *H*$_2$−*H*$_4$ arom.), 10.18 (1H, br, N*H*CO). ^{13}C NMR (CDCl$_3$): δ 18.1, 24.5, 27.0, 27.8, 28.5, 28.7, 29.5, 37.1, 38.5, 40.5, 51.0 (br, *C*B), 53.0, 67.7, 76.6, 79.4, 83.4, 125.0, 125.8, 127.7, 128.4, 130.3, 142.7, 163.363, 177.0. EIMS: *m/z* 424 (M$^+$), 381, 272, 245 (base peak), 228, 203, 131, 93, 67, 55. Anal. Calcd for C$_{24}$H$_{33}$BN$_2$O$_4$: C, 67.90; H, 7.84; N, 6.60. Found: C, 68.32; H, 7.59; N, 6.31.

(+)-Pinanediol (1*R*)-1-(2-Thienylacetylamino)-1-[3-(4,4-dimethyl-4,5-dihydro-oxazol-2-yl)phenyl]methylboronate (**11**). Anhydrous MeOH (1.24 mL of a 2.5 M solution in THF, 3.11 mmol) was added to the solution containing the silylamino derivative **9** and was stirred for 1 h at −10 °C and then for 1 h at rt. The solution was cooled at −78 °C,

2-thiophenacetylchloride (383 μL, 3.11 mmol) in THF (1 mL) was slowly added, and the resulting mixture was allowed to warm to rt overnight. EtOAc (65 mL) and H$_2$O (15 mL) were added, and the aqueous phase was extracted with EtOAc (2 × 15 mL). The combined organic phases were dried (MgSO$_4$) and concentrated to give an orange oil which was purified by gradient chromatography (9:1 EtOAc/EtPet, 95:5 EtOAc/MeOH), affording **11** (360 mg, 25% overall yield from **7**) as a pale orange solid, mp 120 °C, [α]$_D$ = −24.2 (*c* 2.1, CDCl$_3$), de > 98%. IR (KBr): 1646, 1600 cm^{-1}. ^{1}H NMR (CDCl$_3$): δ 0.84 (3H, s, pinanyl C*H*$_3$), 1.23 (1H, d, *J* = 10.5 Hz, pinanyl *H*$_{endo}$), 1.27 (1H, s, pinanyl C*H*$_3$), 1.37 (3H, s, pinanyl C*H*$_3$), 1.38 (3H, s, C*H*$_3$), 1.39 (3H, s, C*H*$_3$), 1.5−2.5 (5H, m, pinanyl protons), 4.13 (1H, br d, *J* = 2.0 Hz, C*H*B), 4.01 (2H, br s, C*H*$_2$CONH), 4.11 (2H, s, C*H*$_2$O), 4.25 (1H, dd, *J* = 8.8, 2.0 Hz, pinanyl C*H*OB), 6.86 (1H, br, N*H*CO), 7.01 (2H, m, CH*CH*CHS−*CH*CS), 7.33 (3H, m, CHC*H*S−*H*$_6$−*H*$_5$ arom.), 7.77 (2H, m, *H*$_2$−*H*$_4$ arom.). ^{13}C NMR (CDCl$_3$): δ 24.8, 27.2, 28.0, 28.58, 28.64, 29.5, 34.3, 36.9, 38.8, 40.6, 48.4 (br, *C*B), 52.9, 67.2, 77.7, 80.7, 84.8, 126.5, 126.7, 126.9, 128.0, 128.7, 129.1, 132.0, 134.6, 142.4, 175.5 (two quaternary *C* not seen). EIMS: *m/z* 506 (M$^+$, base peak), 473, 327, 270, 203, 135, 97, 93, 67, 55. Anal. Calcd for C$_{28}$H$_{35}$BN$_2$O$_4$S: C, 66.40; H, 6.97; N, 5.53; S, 6.33. Found: C, 66.26; H, 7.23; N, 5.29; S, 6.58.

(+)-**Pinanediol (1*R*)-1-{[3-(2-Chlorophenyl)-5-methylisoxazole-4-carbonyl]amino}-1-[3-(4,4-dimethyl-4,5-dihydro-oxazol-2-yl)phen-yl]methylboronate (12).** The boronate **12** was prepared on the same scale following the procedure described for **11** using 3-(2-chlorophenyl)-5-methylisoxazolyl-4-carbonylchloride (796 mg, 3.11 mmol) as the acylating agent. After extraction, the combined organic phases were dried (MgSO$_4$) and concentrated in vacuo to give an orange oil, which was purified by gradient chromatography (Et$_2$O, 95:5 Et$_2$O/MeOH) and triturated with Et$_2$O, affording **12** (276 mg, 16% overall yield from **7**) as a pale yellow solid, mp 140 °C, [α]$_D$ = +182.7 (*c* 2.0, CHCl$_3$), de > 98%. IR (KBr): 1647, 1601 cm^{-1}. ^{1}H NMR (CDCl$_3$): δ 0.83 (3H, s, pinanyl C*H*$_3$), 1.10 (1H, d, *J* = 10.5 Hz, pinanyl *H*$_{endo}$), 1.28 (3H, s, pinanyl C*H*$_3$), 1.33 (3H, s, pinanyl C*H*$_3$), 1.41 (6H, s, 2C*H*$_3$), 1.5−2.5 (5H, m, pinanyl protons), 2.84 (3H, s, C*H*$_3$CON), 4.12 (2H, s, C*H*$_2$O), 4.19 (1H, dd, *J* = 8.8, 2.0 Hz, pinanyl C*H*OB), 4.22 (1H, br d, *J* = 2.4 Hz, C*H*B), 6.10 (1H, br d, *J* = 2.4 Hz, N*H*CO), 7.19 (1H, dt, *J* = 7.5, 1.6 Hz, *H*$_4$ arom.), 7.30 (1H, t, *J* = 7.5 Hz, *H*$_5$ arom.), 7.51 (4H, m, other aromatic protons), 7.67 (1H, m, *J* = 1.6 Hz, *H*$_2$ arom.), 7.78 (1H, dt, *J* = 7.5, 1.6 Hz, *H*$_6$ arom.). ^{13}C NMR (CDCl$_3$): δ 13.8, 24.4, 26.7, 27.8, 28.8 (2*C*), 29.0, 36.2, 38.5, 40.0, 45.2 (br, *C*B), 52.2, 67.9, 78.0, 79.5, 85.6, 126.3, 126.7, 128.0, 128.7, 129.6, 130.9, 131.9, 132.4, 134.4, 140.7, 163.7, 176.2, (isoxazole quaternary *C* not seen). EIMS: *m/z* 601−603 (M$^+$), 566 (base peak), 449, 423−425, 338, 316, 203, 178, 131, 93, 67, 55. Anal. Calcd for C$_{33}$H$_{37}$BN$_3$O$_5$Cl: C, 65.85; H, 6.20; N, 6.98. Found: C, 65.59; H, 6.28; N, 6.83.

General Procedure for the Synthesis of Free Boronic Acids 15−17. The pinanediol esters **10**−**12** (0.30 mmol) were deprotected in degassed HCl (3 N, 7 mL) for 1 h at 120 °C under argon, and the resulting mixture was extracted with EtOAc (2 × 15 mL). The corresponding hydrolysis products **15** and **16** were isolated from the aqueous phase, while compound **17** was isolated from the organic phase.

(1*R*)-1-Acetylamino-1-(3-carboxyphenyl)methylboronic Acid (15). The free boronic acid **15** was isolated from the aqueous phase after removal of the solvent under reduced pressure. Crystallization of the crude residue (boiling acetone) afforded **15** together with an equimolar amount of 2-methyl-2-amino-1-propanol as a light brown solid (58 mg, 59%), mp 90−92 °C. IR (KBr): 3425, 1698, 1620 cm^{-1}. ^{1}H NMR (DMSO): δ 1.20 (6H, s, 2C*H*$_3$), 2.10 (4H, br s, C*H*$_3$CONH−C*H*B), 3.35 (2H, s, C*H*$_2$O), 6.98 (1H, d, *J* = 7.8 Hz, *H*$_6$ arom.), 7.28 (1H, t, *J* = 7.8 Hz, *H*$_5$ arom.), 7.56 (1H, s, *H*$_2$ arom.), 7.69 (1H, d, *J* = 7.8 Hz, *H*$_4$ arom.), 8.02 (3H, br, B(O*H*)$_2$−COO*H*), 9.42 (1H, br, N*H*CO). ^{13}C NMR (DMSO): δ 18.5, 23.1 (2*C*), 31 (br, *C*B), 55.3, 37.3, 126.5, 126.7, 128.3, 130.9, 143.7, 168.5, 176.0. The EIMS was not obtainable.

(1*R*)-1-(2-Thienylacetylamino)-1-(3-carboxyphenyl)methylboronic Acid (16). The free boronic acid **16** was isolated from the aqueous phase after removal of the solvent under reduced pressure. Crystallization of the crude residue (H$_2$O) afforded **16** as an ivory solid (51 mg, 55%), mp 228 °C (dec), [α]$_D$ = −65.5 (*c* 0.5, CH$_3$OH). IR (KBr): 3398, 1704, 1606 cm^{-1}. ^{1}H NMR (CD$_3$OD): δ 3.98 (1H, br s, C*H*B), 4.27 (2H, s, C*H*$_2$CONH), 7.05 (1H, dd, *J* = 5.1, 3.2 Hz, C*H*CHS), 7.19 (1H, br d, *J* = 3.2 Hz, C*H*CS), 7.41 (3H, m, CHC*H*S and *H*$_5$−*H*$_6$ arom.), 7.85 (2H, m, *H*$_2$−*H*$_4$ arom.). ^{13}C NMR (CD$_3$OD): δ 31.0, 53.0 (br, *C*B), 55.3, 126.2, 127.0, 127.2, 127.4, 128.2, 128.4, 130.6, 130.8, 133.5, 141.5, 168.9, 178.5. Anal. Calcd for C$_{14}$H$_{14}$BNO$_5$S: C, 52.69; H, 4.42; N, 4.39; S, 10.05. Found: C, 52.71; H, 4.59; N, 4.31; S, 9.87. The EIMS was not obtainable.

(1*R*)-1-{[3-(2-Chlorophenyl)-5-methylisoxazole-4-carbonyl]amino}-1-(3-carboxyphenyl)methylboronic Acid (17). The free boronic acid **17** was obtained from the organic phase after anhydrification (MgSO$_4$). Removal of the solvent under reduced pressure and crystallization of the crude residue (acetone/Et$_2$O) afforded an ivory solid (82 mg, 50%), mp 180−190 °C, [α]$_D$ = −36.3 (*c* 0.3, CH$_3$OH). IR (KBr): 3409, 1702, 1630 cm^{-1}. ^{1}H NMR (DMSO): δ 2.65 (3H, s, C*H*$_3$CON), 3.58 (1H, br s, C*H*B), 6.90 (1H, d, *J* = 7.2 Hz, *H*$_6$ arom.), 7.11 (1H, t, *J* = 7.2 Hz, *H*$_5$ arom.), 7.50 (8H, m, other aromatic protons−B(O*H*)$_2$), 8.9 (0.5 H, br, N*H*CO), 12.6 (1H, br, COO*H*). ^{13}C NMR (DMSO): δ 12.5, 51.0 (br, *C*B), 125.7, 126.2, 126.7, 127.3, 127.4, 129.7, 129.8, 130.4, 131.5, 131.6, 131.7, 132.6, 142.6, 159.2, 163.8, 167.5, 172.8. Anal. Calcd for C$_{19}$H$_{16}$BClN$_2$O$_6$: C, 55.04; H, 3.89; N, 6.76. Found: C, 54.91; H, 4.03; N, 6.51. The EIMS was not obtainable.

(+)-Pinanediolphenylboronate (19). A solution of (+)-pinanediol (665 mg, 3.9 mmol) and phenylboronic acid (**18**) (476 mg, 3.9 mmol) in THF (5 mL) was stirred for 10 min, concentrated, and distilled to yield **21** (879 mg, 88%), bp 135 °C (1.5 mmHg) as a viscous colorless oil which solidified on standing, mp 50 °C, [α]$_D$ = +14.9 (*c* 2.3, CHCl$_3$). IR (KBr): 2910, 1361, 1094, 701 cm^{-1}. ^{1}H NMR (CDCl$_3$): δ 0.92 (3H, s, pinanyl C*H*$_3$), 1.25 (1H, d, *J* = 10.5 Hz, pinanyl *H*$_{endo}$), 1.34 (3H, s, pinanyl C*H*$_3$), 1.50 (3H, s, pinanyl C*H*$_3$), 1.9−2.6 (5H, m, pinanyl protons), 4.48 (1H, dd, *J* = 8.8, 2.0 Hz, pinanyl C*H*OB), 7.34−7.54 (3H, m, *H*$_m$−*H*$_p$), 7.85 (2H, dd, *J* = 7.9 Hz, 1.6, *H*$_o$). ^{13}C NMR (CDCl$_3$): δ 24.4, 26.9, 27.5, 29.1, 36.0, 38.6, 40.0, 51.9, 78.7, 86.6, 128.1, 131.5, 135.2. Aromatic *C*B not seen. EIMS: *m/z* 256 (M$^+$), 241, 215, 187, 173, 108 (base peak), 93, 77. Anal. Calcd for C$_{16}$H$_{21}$BO$_2$: C, 75.02; H, 8.26. Found: C, 74.77; H, 8.53.

(+)-Pinanediol (1*R*)-1-(2-Thienylacetylamino)-1-phenylmethylboronate (20). The product was synthesized from **19** (700 mg, 2.73 mmol) following the procedure described for **11**. The crude residue was purified by chromatography (7:3 EtPet/EtOAc), affording **20** as a white solid (631 mg, 56% overall yield), mp 50−55 °C, [α]$_D$ = +7.1 (*c* 2.4, CHCl$_3$), de > 98%. IR (KBr): 1602 cm^{-1}. ^{1}H NMR (CDCl$_3$): δ 0.80 (3H, s, pinanyl C*H*$_3$), 1.15 (1H, d, *J* = 10.5 Hz, pinanyl *H*$_{endo}$), 1.23 (3H, s, pinanyl C*H*$_3$), 1.35 (3H, s, pinanyl C*H*$_3$), 1.4−2.5 (5H, m, pinanyl protons), 3.97 (2H, br s, C*H*$_2$CONH), 4.06 (2H, br s, C*H*B), 4.22 (2H, dd, *J* = 8.8, 2.0 Hz, pinanyl C*H*OB), 6.53 (1H, br, N*H*CO), 7.00 (2H, m, C*H*CHS−*H*$_p$), 7.18 (3H, m *H*$_m$−C*H*S), 7.26 (3H, m C*H*CS−*H*$_o$). ^{13}C NMR (CDCl$_3$): δ 24.8, 27.0, 27.9, 29.3, 35.2, 36.7, 38.8, 40.5, 47.5 (br, *C*B), 52.7, 78.0, 85.4, 126.8, 126.9, 127.0, 128.3, 128.8, 129.1, 135.3, 140.9, 174.3. EIMS: *m/z* 409 (base peak, M$^+$), 394, 376, 340, 311, 284, 257, 230, 173, 117, 97, 91, 69. Anal. Calcd for C$_{23}$H$_{28}$BNO$_3$S: C, 67.48; H, 6.89; N, 3.42; S, 7.83. Found: C, 67.21; H, 7.01; N, 3.36; S, 7.52.

(1*R*)-1-(2-Thienylacetylamino)-1-phenylmethylboronic Acid (21). The product was synthesized from **20** (387 mg, 0.95 mmol) following the protocol described for **15**−**17**. The combined aqueous phases were concentrated, affording the free boronic acid **21** as an ivory solid (103 mg, 58%.), mp 90−100 °C, [α]$_D$ = −3.1 (*c* 2.1, CD$_3$OD). IR (KBr): 3420, 1628 cm^{-1}. ^{1}H NMR (CD$_3$OD): δ 3.82 (1H, br s, C*H*B), 4.16 (2H, br s, C*H*$_2$CONH), 6.98−7.32 (7H, m, C*H*CHS−C*H*CS−*H*$_o$−*H*$_m$−*H*$_p$), 7.38 (1H, dd, *J* = 5.3, 1.0 Hz, CHC*H*S). ^{13}C NMR (CD$_3$OD): δ

30.9, 53.4 (br, *C*B), 125.7, 125.9, 126.0, 127.3, 128.0, 128.1, 129.0, 133.6, 178.0. Anal. Calcd for C$_{13}$H$_{14}$BNO$_3$S: C, 56.75; H, 5.13; N, 5.09; S, 11.65. Found: C, 56.53; H, 5.07; N, 4.90; S, 11.57. The EIMS was not obtainable.

Enzymology. The phenylglycylboronic acids were dissolved in DMSO at a concentration of 50 mM; more dilute stocks (10 mM to 1 μM) were subsequently prepared as necessary. Kinetic measurements were performed using nitrocefin as substrate in 50 mM Tris buffer, pH 7.0, and monitored in an HP8453 UV−vis spectrophotometer. The concentration of AmpC was determined spectrophotometrically in stock solutions made from lyophilized powder; this enzyme had been previously expressed and purified.[25] The concentration of enzyme in all reactions was 1.75 nM, except when assaying compound **16**, where the concentration used was reduced 2- to 4-fold (the results from the 0.8 nM enzyme concentration reactions are reported here). To determine K_i values, inhibitor and enzyme were incubated together at their final concentration in the cuvettes for 5 min before the reaction was initiated by the addition of 200 μM substrate. K_i values for compounds **15**, **16**, **17**, and **21** were obtained by comparison of progress curves in the presence and absence of inhibitor, using the method described by Waley,[34] which has been widely used for boronic acid inhibitors of β-lactamases. In these analyses, sufficient inhibitor was used to give at least 50% inhibition; the K_i values reported are the averages calculated from reactions at six different inhibitor concentrations, each of which was repeated three times. The lowest concentration of the 1 nM inhibitor **16** in these assays was 3 nM. Because this concentration approaches that of enzyme, inhibition values for these reactions were checked against reactions run with enzyme at 0.4 nM to ensure that the measured inhibition values were not significantly perturbed by the enzyme's effect on free inhibitor concentration. In all reactions, rates were measured after reactions had overcome their initial lag phase and had reached a steady state.

The selectivity of compounds **16** and **21** was tested by determining their activity against the serine proteases α-chymotrypsin (bovine pancreatic), β-trypsin (bovine pancreatic), and elastase (porcine pancreatic), all from Sigma (St. Louis, MO). The substrates for α-chymotrypsin (succinyl-Ala-Ala-Pro-Phe-*p*-nitroanilide) and β-trypsin (*N*-benzoyl-L-arginine ethyl ester) were also purchased from Sigma. The elastase substrate (MeOSuc-Ala-Ala-Pro-Val-*p*NA) was purchased from Calbiochem (San Diego, CA). Substrates were diluted from 20 mM DMSO stock solutions, and all reactions were performed in 50 mM Tris buffer, pH 7.0, 25 °C. For α-chymotrypsin, 0.001 mg/mL enzyme and the inhibitor at its final concentration were incubated in the cuvette for 5 min before the reaction was initiated by the addition of 200 μM substrate. The reaction was monitored at 410 nm. For β-trypsin, 0.004 mg/mL enzyme and the inhibitor at its final concentration were incubated in the cuvette for 5 min before the reaction was initiated by the addition of 200 μM substrate. The reaction was monitored at 253 nm. For elastase, 0.006 mg/mL enzyme and the inhibitor at its final concentration were incubated in the cuvette for 5 min before the reaction was initiated by the addition of 640 μM substrate. The reaction was monitored at 385 nm. Initial rate fits to the absorbance data for the first 100 s were used to determine reaction velocities.

Crystal Growth and Structure Determination. Cocrystals of AmpC in complex with compounds **16** and **21** were grown by vapor diffusion in hanging drops equilibrated over 1.7 M potassium phosphate buffer (pH 8.7) using microseeding techniques. The initial concentration of the protein in the drop was 3.8 mg/mL, and the concentrations of compounds **16** and **21** were 705 μM and 588 μM, respectively. The compounds were added to the crystallization drops in a 1.2% DMSO, 1 M potassium phosphate buffer (pH 8.7) solution. Crystals appeared in 5−7 days after equilibration at 23 °C. Before data collection, crystals were immersed in a cryoprotectant solution of 25% sucrose, 1.7 M

(34) Waley, S. G. *Biochem. J.* **1982**, *205*, 631−633.

potassium phosphate, pH 8.7, for about 30 s, and were flash cooled in liquid nitrogen. Data were measured on the DND-CAT beam line (5IDB) of the Advance Photon Source at Argonne National Lab at 100 K using a Mar-CCD detector. Both data sets were measured from single crystals. Reflections were indexed, integrated, and scaled using the HKL software package.[35] For both structures, the space group was *C*2, with two molecules in the asymmetric unit, each containing 358 residues. The initial phasing model was an AmpC/boronic acid complexed structure (PDB entry 1FSY), with inhibitor, water molecules, and ions removed. The model was positioned by rigid body refinement and refined using the maximum likelihood target in CNS[36] including simulated annealing, positional minimization, and individual B-factor refinement, with a bulk solvent correction. Sigma A-weighted electron density maps were calculated using CNS and used in further steps of manual model rebuilding and placement of water molecules with the program O.[37] The inhibitors were built into the $2|F_o| - |F_c|$ and $|F_o| - |F_c|$ electron density maps in each active site of the asymmetric unit. Subsequent refinement cycles consisted of positional minimization and B-factor refinement in CNS.

Microbiology. Compounds **16** and **21** were tested for synergy with the β-lactam ceftazidime against pathogenic bacteria from clinical isolates at the Hospital Ramón y Cajal; these bacteria were resistant to β-lactams because of the expression of a class C β-lactamase. Strains of bacteria tested were *Citrobacter freundii* mut756-CAZ, *Escherichia coli* 72929 Hip, *E. coli* 4774 Hip (Table 4, *E. coli* 1 and 2, respectively), *Enterobacter cloacae* 72527 ED, *E. cloacae* 8411 CAZ-R clon7, *E. cloacae* 12991 ED (Table 4, *E. cloacae* 1, 2, and 3, respectively), *Pseudomonas aeruginosa* 279/88, and *P. aeruginosa* JMSMA7 (Table 4, *P. aeruginosa* 1 and 2, respectively). Minimum inhibitor concentration (MIC) values were determined with Mueller-Hinton Broth II using the microdilution method according to NCCLS guidelines.[38]

(35) Otwinowski, Z.; Minor, W. *Methods Enzymol.* **1997**, *276*, 307−326.
(36) Brunger, A. T.; Adams, P. D.; Clore, G. M.; DeLano, W. L.; Gros, P.; Grosse-Kunstleve, R. W.; Jiang, J. S.; Kuszewski, J.; Nilges, M.; Pannu, N. S.; Read, R. J.; Rice, L. M.; Simonson, T.; Warren, G. L. *Acta Crystallogr., Sect. D* **1998**, *54*, 905−921.
(37) Jones, T. A.; Zou, J. Y.; Cowan, S. W.; Kjeldgaard, M. *Acta Crystallogr., Sect. A* **1991**, *47*, 110−119.
(38) National Committee for Clinical Laboratory Standards, Methods for dilution antimicrobial susceptibility test for bacteria that grow aerobically. Approved Standard M7-A4; National Committee for Clinical Laboratory Standards: Villanova, PA, 1997; Vol. 17.
(39) Evans, S. V. *J. Mol. Graphics* **1993**, *11*, 134−138.
(40) Ferrin, T. E.; Huang, C. C.; Jarvis, L. E.; Langridge, R. *J. Mol. Graphics* **1988**, *6*, 13−27.